Microwave and Optical Technology Letters

An Interpolated Spatial Images Method for the Analysis of Multilayered Shielded Microwave Circuits

Journal:	*Microwave and Optical Technology Letters*
Manuscript ID:	MOP-08-0071
Wiley - Manuscript type:	Research Article
Date Submitted by the Author:	13-Jan-2008
Complete List of Authors:	Gomez-Diaz, Juan Sebastian; Technical University Cartagena, Communications and Information Technologies Martínez-Mendoza, Mónica; Technical University Cartagena, Communications and Information Technologies Perez Soler, Francisco; Technical University Cartagena, Communications and Information Technologies Alvarez Melcon, Alejandro; Technical University Cartagena, Communications and Information Technologies
Keywords:	Green's Functions, Method of Moments, Multilayered Circuits, Interpolation methods

An Interpolated Spatial Images Method for the Analysis of Multilayered Shielded Microwave Circuits

J. S. Gómez-Díaz, M. Martínez-Mendoza, F. J. Pérez-Soler and A. Álvarez-Melcón

Abstract

In this paper, an efficient interpolation method is presented in order to compute the Green's function associated to electrical sources, when they are placed inside cylindrical cavities. The interpolation scheme is formulated in the frame of the spatial images technique recently developed. The original idea was to calculate, for every location of a point electric source, the complex values of the electric dipole and charge images, placed outside the cavity, to impose the appropriate boundary conditions for the potentials. In order to considerably reduce the computational cost of the original technique, a simple interpolation method is proposed to obtain the complex values of the images for any source location. To do that, a rectangular spatial subdivision inside the cavity is proposed. Each new sub-region is controlled by means of the exact images values obtained when the source is placed at the four corners of the region. The key idea is to use a bilinear interpolation to obtain the images complex values when the source is located anywhere inside this sub-region. The interpolated images provide the Green's functions of the new source positions fast, and with high accuracy. This new approach can be directly applied to analyze printed planar filters. Two examples with CPU time comparisons are provided, showing the high accuracy and computational gain achieved with the technique just derived.

1 Introduction

Nowadays, the accurate analysis of modern microwave systems is fundamental due to their wide use in telecommunication applications. Complex circuits, with high integration degree, operating at high frequencies, and with metallic walls providing shielding to the structures, must be rapidly analyzed. Exact results are also required, so full-wave and precise numerical methods are needed.

In order to analyze these devices, different techniques such as finite elements [1], finite differences [2] or the transmission line matrix method [3] can be used. The main problem of this family of methods is the large quantity of computer resources consumed when the complexity of the circuit increases, entailing large times to obtain the analysis results.

An interesting possibility is to employ the integral equation technique (IE) combined with the Method of Moments (MoM) [4]. In this case, the Green's functions associated with the multilayered shielded medium must be calculated. Two possible formulations can be used to perform this calculation. The first is the spectral domain formulation, which is usually very efficient, but has some convergence problems when the shielding box has large dimensions as compared to the printed circuits dimensions. The second is the spatial domain formulation, which does not have the spectral problems, but still expresses the Green's functions in terms of very slow convergent series of spatial images [5]. As an example, the rectangular enclosure has extensively been analyzed with both techniques (spectral [6] and spatial [5]). The circular enclosure has only been analyzed in the spectral domain [7]. In addition, recent studies have introduced different methods in order to accelerate the Green's functions calculation. The idea is to directly approximate the Green's functions, employing techniques such as interpolation [8] or Neuronal Networks [9]. The main problem of these approaches is that they usually depend on the geometry, structure and frequency range of the problem. When the geometry changes, the numerical parameters of the above methods must be recalculated (for example, a new Neural Network must be re-trained).

In this context, a new spatial domain numerical method for the Green's functions computation was recently proposed in [10] and in [11]. The idea of the method is to use charge

and dipole images outside the cavity to enforce the proper boundary conditions for the potentials. The technique was applied to circular enclosures in [10], and for the first time to more complex shaped enclosures, defined by linear segments, in [11, 12]. The main disadvantage of the spatial images method is that new exact charge and dipole images must be calculated for every electric source point location. This calculation makes the original technique computationally intensive.

In this contribution, we present a new interpolation method for the rapid calculation of the Green's functions, in the frame of the spatial images technique. The idea is not to interpolate the Green's functions, which have fast variations and strong singularities [8, 9], but to do this interpolation in an upper abstraction layer, i.e. interpolating the complex values of the charge and dipole images, which provides the Green's Functions. In this way, the computational cost drastically decreases, so that practical microwave filters can be analyzed fast. The novel technique is based on defining several spatial sub-divisions inside the whole shielding cavity. Each spatial subdivision is controlled by means of the exact images values obtained when the source is placed at the four corners defining the given sub-region. The key idea is to use a bilinear interpolation of the images complex values when the source is located anywhere inside the corresponding sub-region. These new interpolated images provide the Green's functions with high speed and accuracy.

Finally, the usefulness of the new technique just described is demonstrated by analyzing two practical filters, and by comparing its CPU-time with other methods. The first circuit is a square encapsulated band pass printed filter based on coupled-line sections. The filter response is compared to those obtained with a Neural Network (NN) method [9], and with the commercial software ADS©. There is a good agreement in the filter response among the three methods. The second circuit is a 4-poles broadside-coupled filter. In this case, the filter response is obtained with the new interpolated method, and with the commercial software ADS©. Again the agreement among the techniques is very good. The computational cost of the new technique is in all cases very competitive, improving the ADS© computational times, and the Neural Network method (which always requires an additional training time).

2 Theoretical Outline

The basic theoretical details of the new spatial-images technique was presented in [10] and in [11]. In the first paper [10], a spatial-images procedure to obtain the Green's functions inside a circular waveguide was presented. In the second paper [11], a similar strategy was used for the evaluation of the magnetic vector potential and electric scalar potential, due to electric-current sources placed inside enclosures defined by linear segments.

Initially, the technique employs the free-space Green's function in order to impose the appropriate boundary conditions for the fields at discrete points on the lateral cavity walls. For every electric source point, three systems of linear equations must be solved, finding the weights and orientations of both charge and dipole images, which are needed to fulfil the required boundary conditions. To model more complex cavities, the layers of the structure and the top and bottom covers can be taken into account by substituting the free-space Green's functions with the multilayered media Green's functions formulated in the space domain through Sommerfeld integrals [12].

Once the values of the images are computed to impose the proper boundary conditions, the final Green's functions can be recovered with simple finite summations, namely:

$$G_{V_T}(\vec{r},\vec{r}_0') = S_0\left[\tilde{G}_V(\vec{r},\vec{r}_0')\right] + \sum_{k=1}^{N} q_k S_0\left[\tilde{G}_V(\vec{r},\vec{r}_k')\right] \quad (1)$$

$$G_{A_T}^{xx}(\vec{r},\vec{r}_0') = S_0\left[\tilde{G}_A(\vec{r},\vec{r}_0')\right] + \sum_{k=1}^{N} S_k^x S_0\left[\tilde{G}_A(\vec{r},\vec{r}_k')\right] \quad (2)$$

$$G_{A_T}^{yy}(\vec{r},\vec{r}_0') = S_0\left[\tilde{G}_A(\vec{r},\vec{r}_0')\right] + \sum_{k=1}^{N} S_k^y S_0\left[\tilde{G}_A(\vec{r},\vec{r}_k')\right] \quad (3)$$

where $\vec{r}$ is the observation position, $\vec{r}_0'$ is the source location, N is the number of images, S_0 is the Sommerfeld transformation or order zero, q_k are the charge images and ($\vec{S}_k = S_k^x \hat{e}_x + S_k^y \hat{e}_y$) are the complex values of the dipole images. Also, the symbol ($\tilde{G}$) is used to denote spectral domain Green's functions.

The interpolation technique proposed in this paper is based on the smooth behavior of the spatial images complex values, as opposed to the behaviour of the Green's functions, which present strong singularities and fast variations. To show that this is indeed the case, 20 images are used to analyze a square cavity sketched in Fig. 1. The images are situated at fixed points, surrounding the structure. Specifically, they are located at the air-dielectric interface, following the square shape of the structure, and at a distance of 0.5 λ_0 with respect to the cavity walls. For the numerical test, the electric source is varied along the x-axis shown in Fig. 1. The purpose is to study the behaviour of the complex images values when the source moves inside the cavity.

Fig. 2 represents the real and imaginary parts of the computed charge values for the tenth (q_{10}) image, when the source is varied along the x-axis shown in Fig. 1. It is observed that the image values present a smooth variation as a function of the source position. Therefore, their values can be easily recovered from discrete samples, if the Nyquist theorem is fulfilled. A similar study is now performed with the x-component of the magnetic vector potential, using unitary electric current sources. Fig. 3 represents the computed current values for the sixth (S_6^x) dipole image, in a similar situation as before. Also in this case, the response has a smooth behaviour when the source point is placed inside the cavity. All other charges and dipoles of the system of images behave in a similar manner, and are not shown for the sake of space.

Since all the charge and dipole images have a smooth behaviour, the idea is to exactly calculate the complex values for four source positions, which correspond to the corners of a rectangular sub-region. Each source has associated N charges images (q_k) and 2N dipoles images (N oriented along the x-axis (S_x) and N along the y-axis (S_y)). The values of the charge and dipole images at the four corners in a generic rectangular sub-region are shown in Fig. 4. To find the associated images complex values (Q) of an unknown source, placed in an arbitrary position inside the rectangular sub-region (P_{int} in Fig. 4), the bilinear interpolation can be used as follows:

$$Q(P_{\text{int}}) \approx \frac{Q(P1)}{X1\cdot Y1}\cdot X2\cdot Y1 + \frac{Q(P2)}{X1\cdot Y1}\cdot X2\cdot Y2 + \frac{Q(P3)}{X2\cdot Y2}\cdot X1\cdot Y2 + \frac{Q(P4)}{X2\cdot Y2}\cdot X1\cdot Y1 \quad (1)$$

where $Q(P_i)$ denotes the values of the exact charges when the source is placed at the i-th corner of the rectangular sub-region (i = 1, 2, 3, 4). Moreover, X_i and Y_i are the coordinates of the interior source point P_{int}, as shown in Fig. 4. Similar expressions are obtained for the dipole images. The interpolated images provide the Green's functions with high accuracy, and with the advantage that only four exact images values must be calculated to recover the Green's functions inside every defined rectangular sub-region.

The error made with the interpolation method directly depends on the region size (see Fig. 5). In order to evaluate this error, we present the electric scalar potential (G_V) in Fig. 6 and the magnetic vector potential (G_A^{xx}) in Fig. 7, along the observation line shown in Fig. 5, when the source is placed at the position (0.0 λ_0, 0.65 λ_0, 0.1 λ_0) (see Fig. 5). For validation, results from a spectral domain approach [5], only valid for rectangular cavities, are also included. The charge and dipole image values associated to the source are obtained by interpolation. To do that, an interpolation square region (centred at the source position) is defined, and the length of its side (L) is varied (see Fig. 5).

When the length side of the square region is big (L = 0.15 λ_0), the Green's Functions obtained by the interpolated images are not accurate. This is due to the error made by the bilinear interpolation. However, as soon as the area of the square region decreases, the Green's Functions are recovered with higher precision. It can be observed in Fig. 6 and Fig. 7 that convergence is reached for a side of the square region of L = 0.07 λ_0 (with error below 0.05% in both electric scalar and magnetic vector potentials). We have extended this study along the whole cavity, in order to check the maximum length per wavelength of the square region side to obtain an error below 0.1%. In general, convergence is assured when the side of the interpolation region is below L = 0.05 λ_0.

Note that when the source is very close to the cavity walls, a specific spatial images distribution must be employed (see [12]) in order to obtain accurate results. Also, the dipole images values exhibit faster variations in this case, as it can be observed in Fig. 2 and Fig. 3 for sources very close to the walls. Therefore, the interpolation approach is not used when the source is near to the walls (about 0.05 λ_0), in order to avoid very dense sub-regions. Nevertheless, in a practical circuit, most of the mesh cells are not in this situation, and the method proposed can be employed efficiently.

In order to apply the new interpolated Green's Functions to the analysis of practical microwave filters, the integral equation technique solved with the Method of Moments (MoM) method is used. The MoM technique requires a mesh of the planar circuit with about 10 cells per λ_{eff} [4]. The method can also impose a higher constraint in some cases, for example when modelling the singular behaviour of the transversal currents induced on the microstrip lines. The idea proposed in this paper is to use rectangular cells for the discretization of the circuit geometry, and then use their corners to define the sub-regions employed in the interpolation procedure. If the printed circuit is discretized with a different type of cell, other interpolation scheme can be employed. In any case, with the interpolation technique, instead of the millions of systems needed to perform the MoM analysis with the standard spatial images method, only a few systems need to be calculated. During the calculation of the MoM matrix elements, the values of the images for every position of the source are rapidly recovered by interpolation.

In practice, the size of a single microstrip circuit cell can be much smaller than the size of the interpolation sub-region. Then, each sub-region can control several cells, leading to the idea of a multilevel interpolation approach, as illustrated in Fig. 8. This idea will reduce even more the computational cost, when very dense meshes are used in the discretization of the circuits.

The final errors produced using the one-level or the multilevel interpolation approach are very small. For the examples presented in the next section, the differences between the original moment matrix and the matrix obtained with the interpolation technique just derived are always below 0.06%. Moreover, one of the main advantages of the presented technique is that when dense meshes are used, the filling time of the MoM increases almost linearly with the number of cells. This is because the computation of the Green's Function is avoided for each pair of source-observer combinations, and it is only performed at the four corners of each interpolation region.

3 Results

In order to demonstrate the usefulness of the proposed technique, we have analyzed two microwave filters, comparing its CPU-time with other methods. All of the results shown were obtained on a Pentium IV computer with 3.06-GHz processor and a total RAM memory of 2 GB.

When analyzing a microwave filter, a minimum of three rows of cells are needed in the discretization of the printed lines to correctly model the singular behaviour of the currents close to parallel edges. Also, we have used more cells than the strict minimum in the modelling of the printed lines, to obtain high precision in the calculation of the induced currents. Therefore, the sizes of the cells that we use are small, and their side lengths are below the condition $L = 0.05\ \lambda_0$, allowing the use of the multilevel interpolation scheme.

The first example is a 6-poles boxed microstrip band-pass filter based on coupled lines sections sketched in Fig. 9. To analyze this filter, only 12 images are needed to obtain good convergence. The images are placed at fixed points surrounding the structure, as was described in [11], except in those points very close to the walls, where a specific image distribution is employed [12]. Fig. 10 presents the scattering parameters of the filter employing 210 cells, with the new interpolated technique (using a third order interpolation level, see Fig. 8), with the Neural Network method presented in [9], and with the commercial software ADS©. It can be clearly observed that the agreement between the different techniques is good. To measure the computational gain obtained with the new proposed technique, Table 1 shows the CPU-time needed for each method. The original spatial images method obtains the worst time performance, whereas the interpolated technique reaches a very good result. The new method proposed is even faster than the Neuronal Network method, and without the necessity to train a specific network for each different cavity (which spent about 77.4 hours to train in this box). The ADS© time performance is also shown as reference.

Other kind of interesting examples are the broadside-coupled structures for high-performance microwave filters [13]. Fig. 11 shows a 4-poles broadside-coupled filter, which is analyzed with 20 images. The images are again placed at fixed points, surrounding the structure at a distance of $0.5\ \lambda_0$ from the cavity wall, whereas dynamic images positions are used for those points close to the walls. In this case, the images are located at the first air-dielectric interface. A total of 270 cells are used to mesh the printed circuit. Again, all cell length sides are smaller than the condition $L = 0.05\ \lambda_0$, so the multilevel interpolation approach can be employed. The response of the filter analyzed with the original spatial images method, with the proposed interpolation technique (employing the third-order layer level), and with the commercial software ADS© is shown in Fig. 12. Very good agreements between the techniques are obtained, validating the interpolation method. Table 2 presents the CPU times for the three methods. The original spatial images method spent about 1336 seconds per frequency point, showing the practical limitation of this technique. The time increase is due to the number of images employed in this case (20), and to the high complexity of the Sommerfeld integrals used to model the cavity at different levels. The new interpolated method is 98.098% faster than the original technique employing the first-level interpolation, 99.169% with the second-level and 99.682% with the third level, outperforming also the commercial ADS© package.

4 Conclusions

In this paper we have presented a simple acceleration technique for the analysis of printed shielded devices, in the frame of the spatial images formulation. Using this formulation, the relevant Green's functions are recovered from the contribution of a discrete set of spatial images. Instead of calculating the values of the images for every source location, the novel

method proposes to use a bilinear interpolation. The new approach does not use the interpolation at the Green's functions level, since they present singularities and fast variations. Instead, the interpolation is now applied at the charge and dipole images level, because they behave very smoothly. The structure under study is divided into several sub-regions, where the values of the images are calculated using the bilinear interpolation. In each sub-region, the interpolation is controlled by the exact images values calculated when the source is placed at the four corners. Several practical examples are given, showing the accuracy and efficiency of the new proposed technique. The CPU-time performance of the new technique is very good, allowing the analysis, design, and optimization of practical shielded MMIC devices.

Acknowledgement

This work was partially supported by the Spanish Ministry of Education and Science under Grant FPU-AP2006-015 and with the Project TEC2007-67630-C03-02.

References

1. J.-M. Jin and J. L. Volakis, "A finite element-boundary integral formulation for scattering by three-dimensional cavity-backed apertures," IEEE Transactions on Antennas and Propagation, vol. 39, no. 1, pp. 97–104, January 1991.

2. M. Omiya, T. Hikage, N. Ohno, K. Horiguchi, and K. Itoh, "Design of cavity-backed slot antennas using the finite-difference time-domain technique," IEEE Transactions on Antennas and Propagation, vol. 46, no. 12, pp. 1853–1858, December 1998.

3. W. J. R. Hoefer, "The transmission line matrix method; theory and applications," IEEE Transactions on Microwave Theory and Techniques, vol. 33, no. 10, pp. 882–893, October 1985.

4. R. F. Harrington, Field Computation by Moment Methods. Wiley-IEEE Press, 1968.

5. A. A. Melcon and J. R. Mosig, "A novel spatial images technique for the analysis of cavity backed antennas," ACES, Applied Computational Electromagnetics Society, vol. 14, no. 3, March 1999.

6. C. J. Railton and S. A. Meade, "Fast rigorous analysis of shielded planar filters," IEEE Transactions on Microwave Theory and Techniques, vol. 40, no. 5, pp. 978–985, May 1992.

7. F. Zavosh and J. T. Aberle, "Single and stacked circular microstrip patch antennas backed by a circular cavity," IEEE Transactions on Antennas and Propagation, vol. 43, no. 7, pp. 746–750, July 1995.

8. C. H. C. H. G. Wang and L. Tsang, "A new multilevel Green's Function interpolation method for large scale EM simulations in RF ICs," in IEEE, AP-S Antennas and Propagation Intenational Symposium, vol. 2. Monterey, California, USA: IEEE, 20-25, June 2004, pp. 1183 – 1186.

9. J. P. García, F. Quesada-Pereira, D. C. Rebenaque, J. L. G. Tornero, and A. A.Melcón, "A neural network method for the analysis of multilayered shielded microwave circuits," IEEE Transactions on Microwave Theory and Techniques, vol. 54, no. 1, pp. 309 – 320, January 2007.

10. F. Q. Pereira, P. V. Castejón, D. C. Rebenaque, J. P. García, and A. A. Melcón, "Numerical evaluation of the Green's functions for cylindrical enclosures," IEEE Transactions on Microwave Theory and Techniques, vol. 53, no. 1, pp. 94–105, January 2005.

11. J. S. Gómez-Díaz, F. D. Quesada -Pereira, J. L. G. Tornero, J. P. García, and A. Álvarez-Melcón, "Numerical evaluation of the Green's functions for arbitrarily shaped cylindrical enclosures and their optimization by a new spatial images method," Radio Science, vol. 42, no. RS5007, pp. 1–16, October 2007.

12. J. S. Gómez-Díaz, M. Martínez-Mendoza, F. J. Pérez-Soler, F. D. Quesada-Pereira, and A. Álvarez-Melcón, "Practical implementation of the spatial images technique for the analysis of multilayered shielded circuits," IEEE Transactions on Microwave Theory and Techniques, vol. In print, no. 5675, January 2008.

13. A. A. Melcon, J. R. Mosig, and M. Guglielmi, "Broadside couplings for high selectivity microstrip filters," Microwave and Optical Technology Letters, vol. 30, no. 5, pp. 295–302, September 2001.

Table 1: CPU-time comparison for the filter shown in Fig. 9 analyzed with different methods

Spatial Images technique (sec)	80.125
ADS© (sec)	18.691
Neuronal Network (sec)	5.1245
Interpolated method first level (sec)	6.751
Interpolated method second level (sec)	4.822
Interpolated method third level (sec)	2.129

Table 2: CPU-time comparison for the filter shown in Fig. 11 analyzed with different methods

Spatial Images technique (sec)	1336.235
ADS© (sec)	39.234
Interpolated method first level (sec)	18.0519
Interpolated method second level (sec)	9.2237
Interpolated method third level (sec)	3.4521

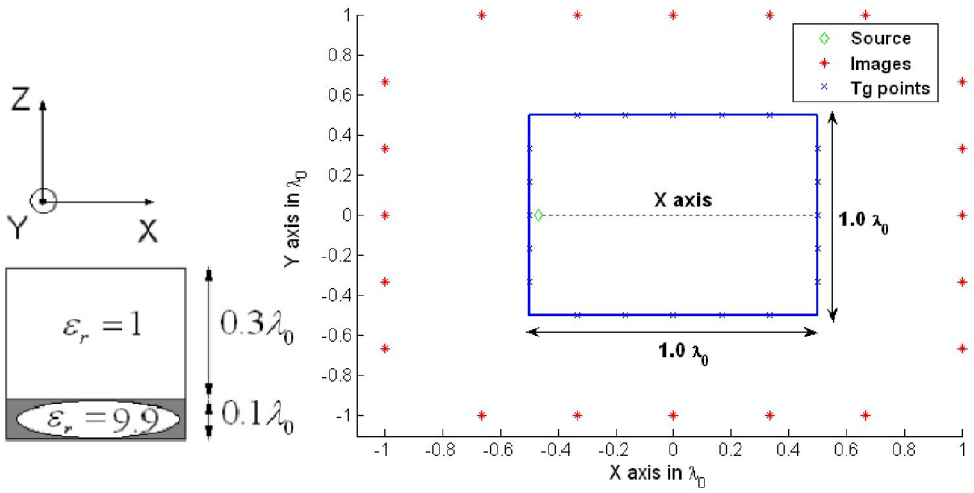

Figure 1: Square cavity used to show the charge/dipole images complex value behaviour.
317x160mm (600 x 600 DPI)

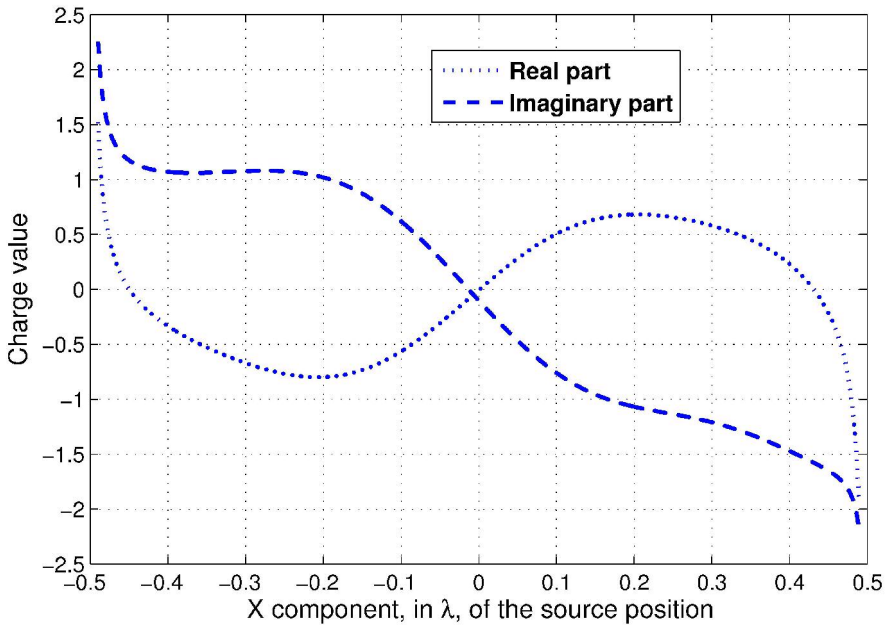

Figure 2: 10th charge image value evolution versus the position of the source inside the box depicted in Fig. 1.
178x120mm (600 x 600 DPI)

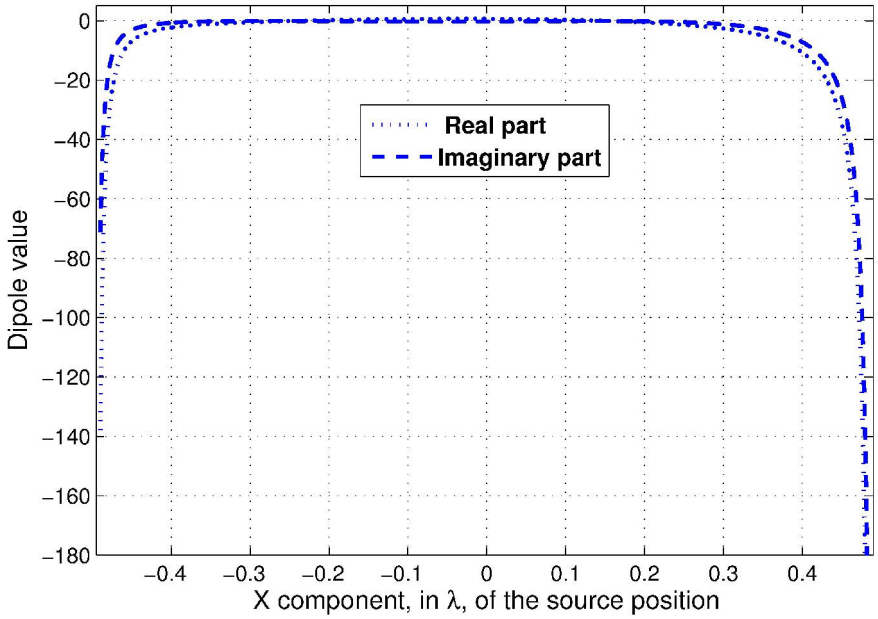

Figure 3: 6th dipole image values evolution versus the position of the source inside the box depicted in Fig. 1.
178x120mm (600 x 600 DPI)

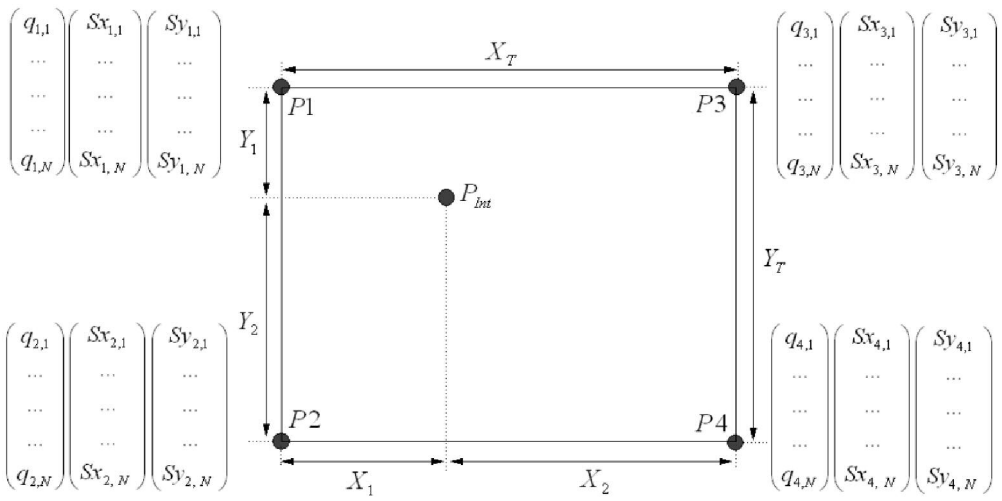

Figure 4: Rectangular interpolation region controlled by four electric-sources placed at the corners.
419x213mm (600 x 600 DPI)

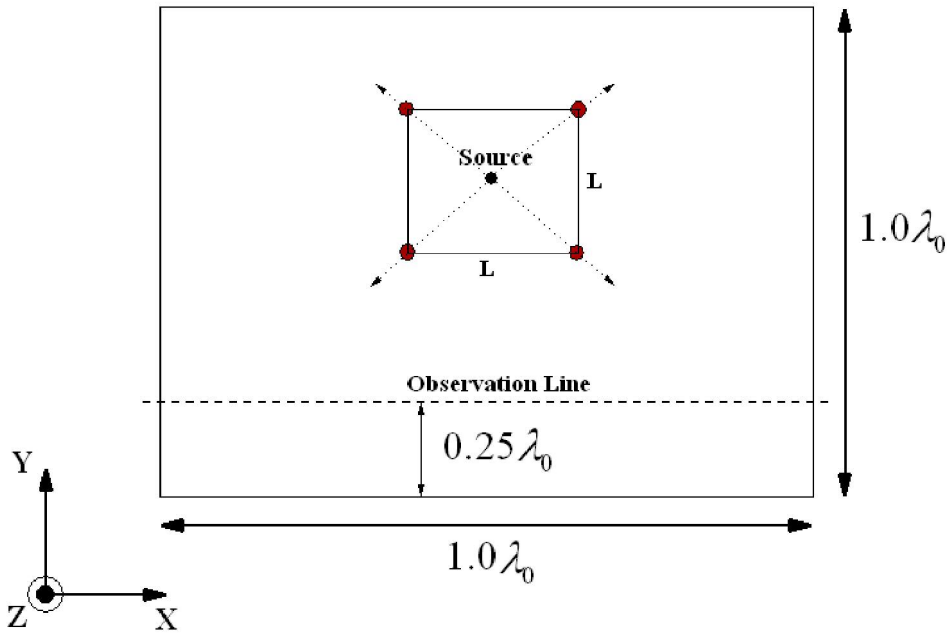

Figure 5: Example of an interpolation square region centred at the source position (0.0 λ0, 0.65 λ0, 0.1 λ0). The length side of the region (L) will change in order to study the interpolation error.
269x186mm (600 x 600 DPI)

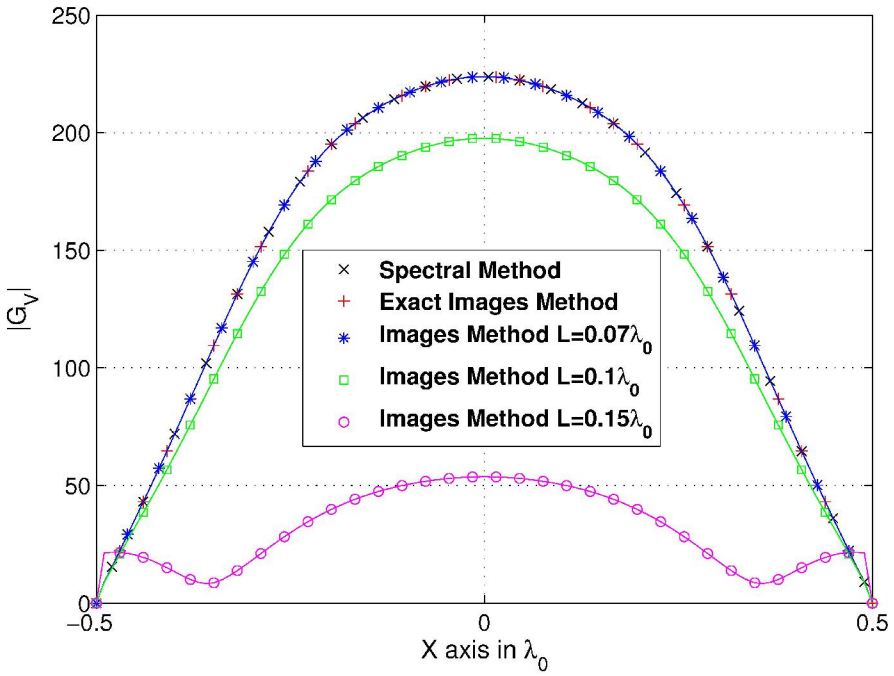

Figure 6: Electric scalar potential ($|G_V|$) along the observation line of Fig. 5, when the side of the square interpolation region has the values of L = 0.15 λ0, L = 0.1 λ0 and L = 0.07 λ0. Data from a spectral method [5] is used as validation.
180x130mm (600 x 600 DPI)

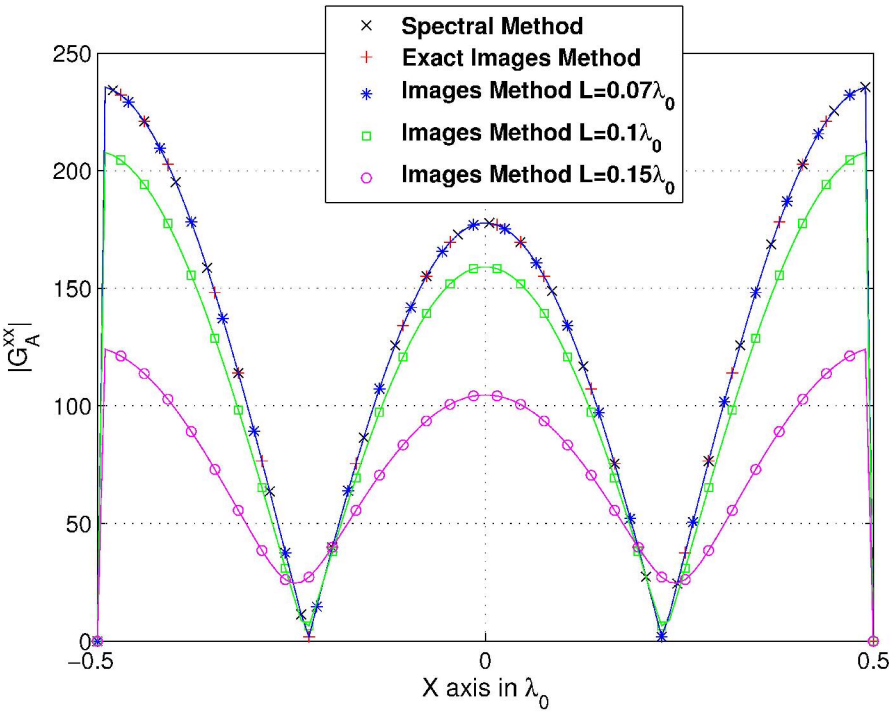

Figure 7: Magnetic vector potential ($|G_A^{xx}|$) along the observation line of Fig. 5, when the side of the square interpolation region has the values of L = 0.15 λ0, L = 0.1 λ0 and L = 0.07 λ0. Data from a spectral method [5] is used as validation.
180x130mm (600 x 600 DPI)

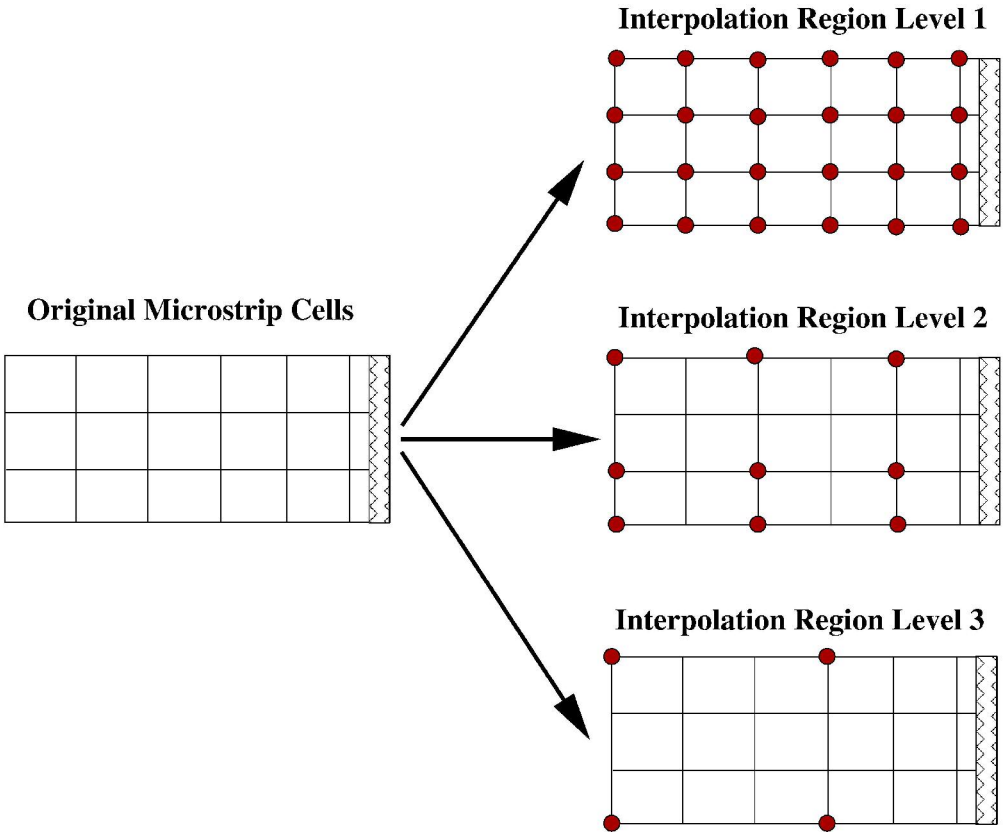

Figure 8: Different interpolation region levels defined over a discretized microstrip line. Region Level 1 controls one cell, Region Level 2 controls four cells and Region Level 3 controls nine cells.
168x140mm (600 x 600 DPI)

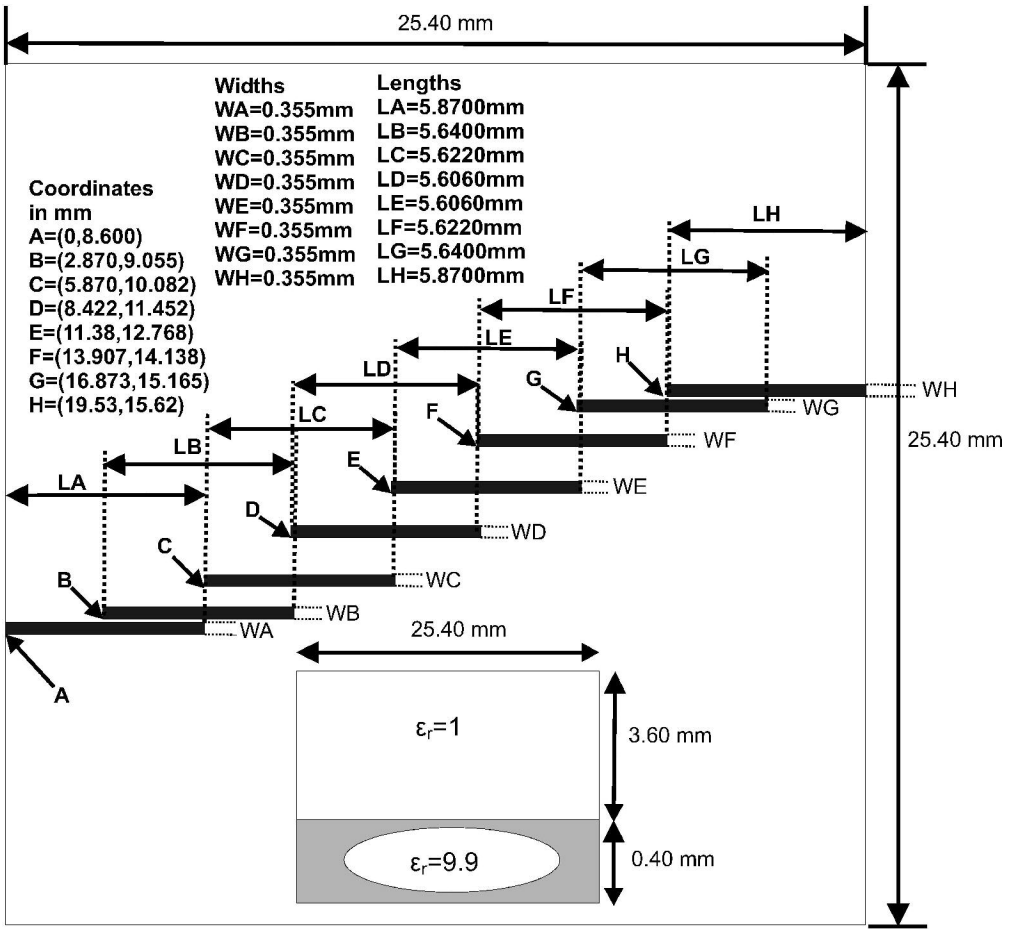

Figure 9: Boxed microstrip 6-poles band-pass filter based on coupled lines sections.
193x178mm (600 x 600 DPI)

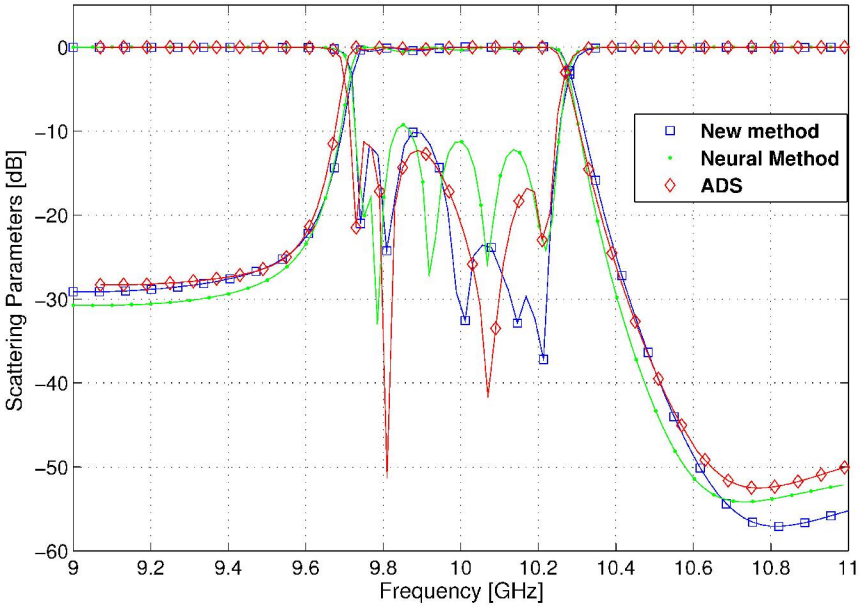

Figure 10: Scattering parameters of the filter shown in Fig. 9 (meshed with 210 cells).
210x141mm (600 x 600 DPI)

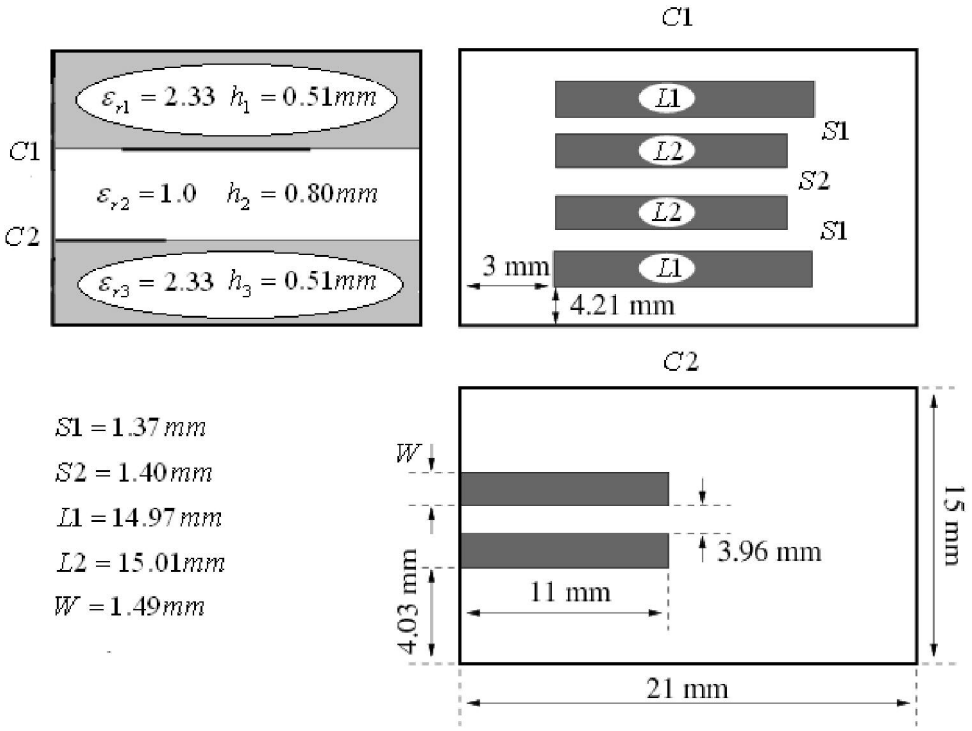

Figure 11: Bandpass broadside-coupled filter.
226x170mm (600 x 600 DPI)

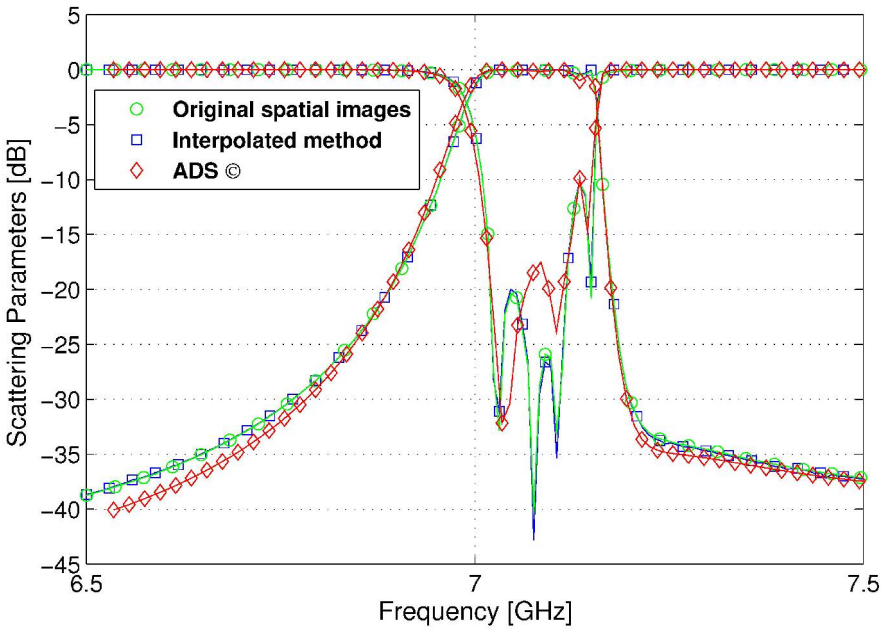

Figure 12: Scattering parameters of the filter shown in Fig. 11 (meshes with 270 cells).
178x120mm (600 x 600 DPI)